

Z-direction B_1^+ Homogenization Using B_1 -control Receive Array Coil and B_1 Rectifying Fin for L-spine Imaging at 3T

Yukio Kaneko¹, Yoshihisa Soutome^{1,2}, Hideta Habara^{1,2}, Yoshitaka Bito², and Hisaaki Ochi¹

¹Central Research Laboratory, Hitachi Ltd., Kokubunji, Tokyo, Japan, ²Hitachi Medical Corporation, Kashiwa, Chiba, Japan

TARGET AUDIENCE RF engineers or scientists with an interest in B_1^+ and local SAR

INTRODUCTION

B_1^+ inhomogeneity in the human body increases as the strength of a static magnetic field increases. Various methods to reduce B_1^+ inhomogeneity have recently been developed, such as dielectric pads [1,2], coupling coils [3-9], and RF shimming [10-13]. However, the B_1^+ inhomogeneity remains in lumbar spine (L-spine) imaging, especially in the direction of z-axis (axis of the body). A dark signal appears in the region of the spine, or the effect of fat suppression near the spine is not sufficient. Our previous study showed that a “ B_1 -control receive array coil (BRAC) [14]” and “ B_1 rectifying fin (BRF) [15]” can control the B_1^+ field locally. These techniques can potentially reduce B_1^+ inhomogeneity in the z-direction. In this study, the BRAC and BRF around a human model were designed in an FDTD simulator, and the B_1^+ field and local SAR field were calculated. It was confirmed that the BRAC and BRF can reduce B_1^+ inhomogeneity in the z-direction.

METHOD

Principle: The magnetic flux around a conductive loop or fin (loop/fin) is shown schematically in Figure 1. The loop/fin, whose resonance frequency is sufficiently lower than the transmit RF frequency, exhibits inductive characteristics (inductive mode). The flux density decreases around the center of the loop/fin and increases near the edge of the loop/fin. The spatial distribution of the flux density around the loop/fin can compensate for the B_1^+ inhomogeneity. A circuit schematic of a BRAC is shown in Figure 2. Unlike a conventional receive array coil, additional PIN diodes (D_1) are connected in parallel to the capacitors of the BRAC. The conventional coil only has a detuning mode during the RF transmit period. On the other hand, the BRAC has both detuning and inductive modes, and these two modes can be switched. BRF has the same function for changing the magnetic flux, because an electrical current flows in a direction that counters the magnetic flux across the fin.

Simulation: The effect of the BRAC and BRF was clarified through numerical analysis of the B_1^+ and local SAR field using an electromagnetic simulation tool (CST Microwave StudioTM). The simulation model of the 32-channel BRAC is shown in Figure 3. Sixteen loops (rows 2 and 3) were used in the inductive mode, and the others were used in the detuning mode. A 2-channel birdcage coil was used for RF transmission, and the RF frequency was 128 MHz. The diameter of the birdcage coil was 700 mm, and the length of the rungs was 520 mm. Hugo (height: 180 cm, weight: 90.3 kg) was used as a human model. Hugo's arms were repositioned from the side of its body to above its head. The landmark position was set at the L-spine in the z-direction. Each loop was made of a copper sheet, and the loop size was 170 x 170 mm. The simulation model of the BRF is shown in Figure 4. The copper mesh sheet was modeled and positioned around the L-spine region. The length of the sheet in the z-direction was 330 mm. The position of the Region Of Interest (ROI) is shown in Figure 5. The ROI includes the L-spine region. The value of B_1^+ homogeneity (U_{SD}) was defined as $U_{SD} = \sigma / \bar{B}_1$, where σ is the standard deviation of B_1^+ and \bar{B}_1 is the average of B_1^+ in a sagittal slice at $x = 0$ mm. The maximum local SAR was defined as the maximum value of 10g SAR in the body. RF transmission mode was quadrature (QD) drive or 2-channel RF shimming, and U_{SD} was minimized in RF shimming.

RESULTS

The B_1^+ maps in the human model are shown in Figure 6. Case (a) represents the B_1^+ map obtained in QD drive; case (b) represents that obtained in RF shimming; case (c) represents that obtained with BRAC in QD drive; case (d) represents that obtained with BRAC in RF shimming; case (e) represents that obtained with BRF in QD drive; and case (f) represents that obtained with BRF in RF shimming. The \bar{B}_1 was normalized to 1 μ T. B_1^+ inhomogeneity remains in case (b), in which RF shimming alone was used. The B_1^+ inhomogeneity is decreased by using BRAC or BRF. The U_{SD} , whole-body SAR (WB SAR), and maximum local SAR for each case are shown in Figure 7. The U_{SD} in the case of the RF shimming with BRAC (case (d)) is 20 % less than that in the case of RF shimming alone (case (b)). The U_{SD} in the case of the RF shimming with BRF (case (f)) is 35 % less than that in the case of RF shimming alone (case (b)).

DISCUSSION

It is considered that the reason why the effect is different between the BRAC and the BRF is the scale of the electrical current. The BRAC consists of several small loops, while the BRF consists of one large sheet. Therefore, the BRF generates a larger-scale current than the BRAC. It is indicated that the current scale generated by BRF is more effective for the B_1^+ homogenization than that by BRAC in this situation of the L-spine imaging. Recently, some papers have described the effect of z-shim RF array coil [12,13] and how the B_1^+ inhomogeneity is decreased by using multi-channel coils in the z-direction. The BRAC and BRF can potentially reduce B_1^+ inhomogeneity in the z-direction without the increase of the number of RF transmit channel. Note that when BRF is used for L-spine imaging, the receive array coil has to be set near the human body. Thus, the receive array coil is set between the human body and BRF, for example.

CONCLUSION

It is shown that a B_1 -control receive array coil (BRAC) and B_1 rectifying fin (BRF) can reduce B_1^+ inhomogeneity in the L-spine imaging. Using the BRAC and BRF is more effective than RF shimming alone in reducing B_1^+ inhomogeneity, and BRF can potentially reduce maximum local SAR.

REFERENCES

- [1] Schmitt M. et al. ISMRM 2004; 11: 197.
- [2] Kendra M.F. et al. J Magn Reson Imaging 2008; 27: 1443-1447.
- [3] Schmitt M. et al. ISMRM 2005; 13: 331.
- [4] Wang S. et al. ISMRM 2007; 15: 3275.
- [5] Wiggins G.C. et al. ISMRM 2007; 15: 1054.
- [6] Wang S. et al. IEEE Trans Med Imag 2010; 28: 551.
- [7] Sacolick L. et al. ISMRM 2010; 18: 3809.
- [8] Hancu I. et al. ISMRM 2010; 18: 2470.
- [9] Merkle H. et al. MRM 2011; 66: 901.
- [10] Nistler J. et al. ISMRM 2007; 15: 1063.
- [11] Hajnal J.V. et al. ISMRM 2008; 16: 496.
- [12] Wu X. et al. ISMRM 2013; 21: 4398.
- [13] Tian J. et al. ISMRM 2013; 21: 2746.
- [14] Kaneko Y. et al. ISMRM 2012; 20: 2611.
- [15] Kaneko Y. et al. ISMRM 2010; 18: 3810.

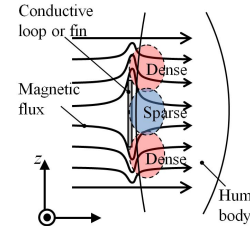


Fig.1: Magnetic flux around a conductive loop or fin.

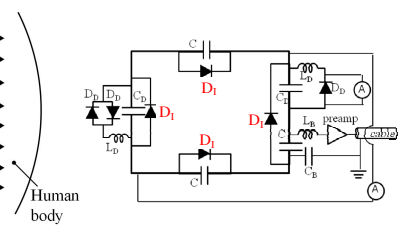


Fig.2: Circuit of BRAC.

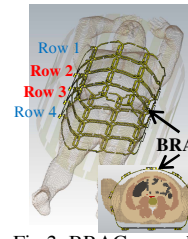


Fig.3: BRAC around the human body.

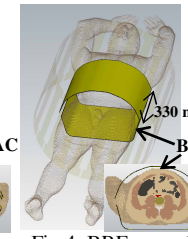


Fig.4: BRF around the human body.

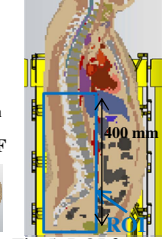


Fig.5: ROI for B_1^+ homogenization.

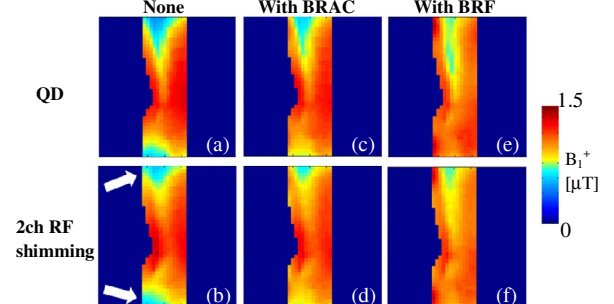


Fig.6: B_1^+ maps in the human model: (a) QD drive (b) RF shimming alone (c) QD with BRAC (d) RF shimming with BRAC (e) QD with BRF (f) RF shimming with BRF.

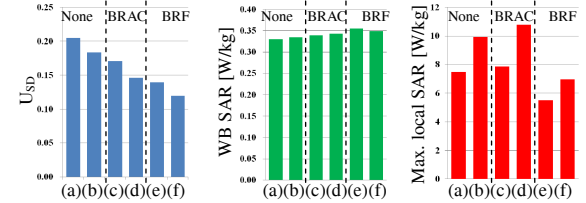


Fig.7: U_{SD} , WB SAR, and maximum local SAR for each case.